A practical solution to the shape optimization problem of solid structures

M. Shimoda[1], S. Motora[2] & H. Azegami[3]
[1]*Department of Mechanical Design Engineering, Shonan Institute of Technology, Japan*
[2]*Graduate School of Shonan Institute of Technology, Japan*
[3]*Nagoya University, Japan*

Abstract

This paper presents a practical optimization method for the shape design of solid structures or 3-dimensional structures in order to obtain the optimal free boundary shape without any parameterization of the shape for optimization. A solution to the rigidity design problem of a solid structure under the assumption that the Neumann boundary is allowed to vary is presented. The compliance is minimized subject to a volume constraint and the state equation. Surface tractions, body forces and hydrostatic pressure are applied on the specified regions. This design problem is formulated as a non-parametric shape optimization problem. The shape gradient function is theoretically derived using the Lagrange multiplier method, the material derivative method and the adjoint variable method. With the shape gradient function and the traction method that was proposed by the authors as a gradient method in a Hilbert space, the smooth optimal shape can be easily obtained. This solution is applied to four design problems. The results obtained verified the effectiveness and practical utility of the proposed method for the shape design of solid structures with variable Neumann boundaries.
Keywords: solid structure, shape optimization, traction method, optimal shape, non-parametric optimization, adjoint variable, material derivative.

1 Introduction

Solid, 3-dimensional structures are widely used in the mechanical and structural components of human-made objects such as vehicles, electrical appliances and

www.witpress.com, ISSN 1743-3509 (on-line)
doi:10.2495/OP090041

architectures. Determining the optimal shape of components is a universal problem in all areas of mechanical and structural design. Product performance requirements for weight, cost, rigidity, strength, vibration and other attributes are becoming increasingly severe because of issues related to the depletion of natural resources and environmental protection. The development of shape optimization techniques is essential in order to obtain solutions efficiently and economically, as well as to overcome the limitations of current designs. In the shape design of solid components in particular, the optimal free-form design is required in order to fulfill the design requirements because solid structures have many design degrees of freedom. We have developed a non-parametric shape optimization method, which we call the "traction method" [1], and applied it to various shape design problems of 2D and 3D continua including plate and shell structures in our previous studies [2-3]. In optimizing a solid structure using a parametric shape optimisation method like the basis vector method, which is one of the best shape optimization techniques, we often encounter the problem of how to parameterize the shape or the problem of how to prepare the basis vectors. How many and which basis vectors are the best for obtaining the optimal shape? The result obtained also strongly depends on the basis vectors used. In contrast, with the traction method, we can easily obtain the smooth optimal boundary shape without any parameterization of the shape.

In this study, we applied the traction method to the shape optimization of solid structures under the assumption that the Neumann boundary was allowed to vary. It is important for structural designers to optimize the Neumann boundary for reducing the total amount of applied loads. The traction method is a gradient method in a Hilbert space. This study considered the rigidity design problem of a solid structure with variable Neumann boundaries. Surface tractions, body forces and hydrostatic pressure were applied on the specified regions. The compliance was minimized subject to a volume constraint and the state equation. The sensitivity function, i.e., the shape gradient function, and the optimality conditions for this problem were derived using the Lagrange multiplier method, the material derivative method and the adjoint variable method. In the traction method, the negative shape gradient function is applied in the normal direction to the design surface as an external force to vary the shape. This method was applied to four design problems involving a beam, a dam and a tower. The effect of each term in the shape gradient function on the optimum shape was also evaluated. The validity and practical utility of this method for the optimum shape design of solid structures with variable Neumann boundaries were verified by the results obtained.

2 Domain variation and material derivative for optimization

A technique for representing domain variation using the speed method [4] will be introduced briefly before formulating the shape optimization problem. A detailed explanation of this technique may be found in references [1] and [5].

As shown in Fig. 1, it is assumed that a linear elastic body having an initial domain of $\Omega \subset \mathbb{R}^3$ and boundary of $\Gamma \equiv \partial\Omega$ undergoes variation (i.e., the design velocity field) V such that its domain and boundary become Ω_s and Γ_s. The notation $\mathbb{R}$ indicates a set of positive real numbers. The domain variation can be expressed by a one-to-one mapping $T_S(\boldsymbol{X}) : X \in \Omega \mapsto x \in \Omega_S$, $0 \le s < \varepsilon$. The notation s and ε indicate the iteration history of domain variation and a small positive number, respectively. Assuming a constraint is acting on the variation in the domain $\Theta \subset \Omega$, the infinitesimal variation of the domain can be given by

$$T_{s+\Delta s}(\boldsymbol{X}) = T_s(\boldsymbol{X}) + \Delta s \boldsymbol{V} \ , \tag{1}$$

where the design velocity field $\boldsymbol{V}$ is given as a derivative of $T_s(\boldsymbol{X})$ with respect to s and can be defined as a continuous function as

$$\boldsymbol{V}(\boldsymbol{x}) = \frac{\partial T_s}{\partial s}(T_s^{-1}(\boldsymbol{x})), \ \ \boldsymbol{x} \in \Omega_s \ , \tag{2}$$

$$\boldsymbol{V} \in C_\Theta = \{\boldsymbol{V} \in C^1(\Omega; \mathbb{R}^3) \,|\, \boldsymbol{V} = \boldsymbol{0} \text{ in } \Theta\} \, . \tag{3}$$

The derivative of a response functional is obtained as indicated below. When a response functional J is given as a domain integral of a distributed function ϕ_s,

$$J = \int_{\Omega_s} \phi_s d\Omega \ . \tag{4}$$

The material derivative with respect to s $\dot{J}$ is given by the following expression.

$$\dot{J} = \int_{\Omega_s} \phi_s' d\Omega + \int_{\Gamma_s} \phi_s V_n d\Gamma \ , \tag{5}$$

where $V_n = n_i V_i$. The vector $\boldsymbol{n}$ is an outward unit normal vector. The notation $(\cdot)'$ indicates a shape (Lagrange) derivative with respect to s [4]. When a response functional J is given as a boundary integral of a distributed function ϕ_s,

$$J = \int_{\Gamma_s} \phi_s d\Gamma \, , \tag{6}$$

the material derivative $\dot{J}$ is given by

$$\dot{J} = \int_{\Gamma_s} \{\phi_s' + (\phi_{s,i} n_i + \phi_s \kappa) V_n\} d\Gamma \ , \tag{7}$$

where κ expresses the mean curvature when it is three dimensional.

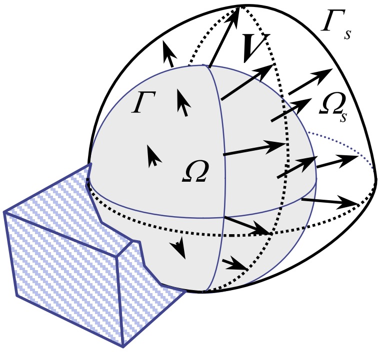

Figure 1: Domain variation by $\boldsymbol{V}$.

The tensor notation employed in this paper uses Einstein's summation convention and a partial differential notation $(\cdot)_{,i} = \partial(\cdot)/\partial x_i$.

3 Formulation of shape optimization problem of solid structure

The non-parametric shape optimization problem for the rigidity design of a solid structure with linear elastic material is solved. Consider body forces per unit volume $\boldsymbol{f}(\boldsymbol{x})$, surface forces per unit area $\boldsymbol{P}(\boldsymbol{x})$ and pressure $p(\boldsymbol{x})\boldsymbol{n}$ act on Ω, Γ_1 and Γ_2, respectively. Letting $l(\boldsymbol{v})$ denote the compliance as an index of rigidity, the rigidity design problem or the compliance minimization problem subject to constraints of volume and the state equation can be formulated as shown below.

$$\text{Find} \quad \Omega_s \quad (\text{or } \boldsymbol{V}), \tag{8}$$

$$\text{that minimize} \quad l(\boldsymbol{v}), \tag{9}$$

$$\text{subject to} \quad a(\boldsymbol{v},\boldsymbol{w}) = l(\boldsymbol{w}), \quad \forall \boldsymbol{w} \in U, \tag{10}$$

$$M \left(= \int_{\Omega_s} d\Omega\right) \le M_0 , \tag{11}$$

where M and M_0 denote the volume and its constraint value. The bilinear form $a(\boldsymbol{v},\boldsymbol{w})$ that gives the variational strain energy and the linear form $l(\boldsymbol{w})$ that gives the variational potential energy due to the external force are defined as

$$a(\boldsymbol{v},\boldsymbol{w}) = \int_{\Omega} e_{ijkl} v_{k,l} w_{i,j} d\Omega , \tag{12}$$

$$l(\boldsymbol{w}) = \int_{\Omega} f_i w_i d\Omega + \int_{\Gamma_1} P_i w_i d\Gamma + \int_{\Gamma_2} p(\boldsymbol{x}) n_i w_i d\Gamma , \tag{13}$$

where $\boldsymbol{v}$, $\boldsymbol{w}$ and e_{ijkl} are the displacement vector, the variational displacement vector and the elastic coefficients, respectively, and U denotes the suitably smooth function space that satisfies the displacement constraint condition.

Letting $\boldsymbol{w}$ and Λ denote the Lagrange multipliers for the state equation and the volume constraint, respectively, the Lagrangian functional L for this problem can be expressed as

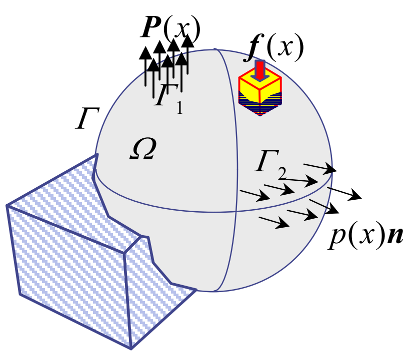

Figure 2: Boundary condition.

$$L(\Omega, \boldsymbol{v}, \boldsymbol{w}, \Lambda) = l(\boldsymbol{v}) - a(\boldsymbol{v}, w) + l(\boldsymbol{w}) + \Lambda(M - M_0) . \tag{14}$$

Assuming that the body forces and the surface forces are constant with respect to s within the space ($\boldsymbol{f}' = \boldsymbol{P}' = 0$) and that the material is homogeneous and constant ($\dot{e}_{ijkl} = e'_{ijkl} = 0$), the material derivative $\dot{L}$ with respect to the domain variation of the Lagrangian functional L is expressed using the design velocity field $\boldsymbol{V}$ as follows:

$$\dot{L} = l(\boldsymbol{v}') - a(\boldsymbol{v}', \boldsymbol{w}) - a(\boldsymbol{v}, \boldsymbol{w}') + l(\boldsymbol{w}') + \Lambda'(M - M_0) + l_G(\boldsymbol{V}) , \tag{15}$$

$$l_G(\boldsymbol{V}) = \int_\Gamma \{f_i(v_i + w_i) - e_{ijkl} v_{k.l} w_{i,j} + \Lambda) V_n d\Gamma$$
$$+ \int_{\Gamma_1} [\{P_{i,j} n_j (v_i + w_i) + P_i (v_{i,j} + w_{i,j}) n_j + P_i (v_i + w_i) \kappa\} V_n] d\Gamma$$
$$+ \int_{\Gamma_2} [p'(v_i + w_i) n_i + \mathrm{div}(p v_i + p w_i) V_n] d\Gamma \ . \tag{16}$$

The optimality conditions of this functional L with respect to $\boldsymbol{v}$, $\boldsymbol{w}$ and Λ are expressed as shown below.

$$a(\boldsymbol{v}, \boldsymbol{w}') = l(\boldsymbol{w}'),\ \forall \boldsymbol{w}' \in U \ , \tag{17}$$

$$a(\boldsymbol{v}', \boldsymbol{w}) = l(\boldsymbol{v}'),\ \forall \boldsymbol{v}' \in U \ , \tag{18}$$

$$\Lambda(M - M_0) = 0,\ \ M - M_0 = 0,\ \ \Lambda \geq 0 \ , \qquad (19)(20)(21)$$

where eqn. (17) is the governing equation of $\boldsymbol{v}$ which coincides with the state eqn. (10), and eqn. (18) is the governing equation of $\boldsymbol{w}$. The Lagrange multiplier Λ is determined so as to satisfy eqns. (19)–(21). Further, a comparison of governing eqn. (17) and adjoint eqn. (18) yields the following self-adjoint relationship:

$$\boldsymbol{v} = \boldsymbol{w} \ . \tag{22}$$

By substituting $\boldsymbol{v}$ (or $\boldsymbol{w}$) into eqn. (15), the material derivative $\dot{L}$ can be expressed as the dot product of the shape sensitivity function (i.e., shape gradient function) $\boldsymbol{G}$ and the design velocity field $\boldsymbol{V}$ as shown in eqns. (23)–(26).

$$\dot{L} = l_G(\boldsymbol{V}) \equiv \int_\Gamma G\boldsymbol{n} \cdot \boldsymbol{V} d\Gamma \equiv \int_\Gamma \boldsymbol{G} \cdot \boldsymbol{V} d\Gamma$$
$$= \int_\Gamma \boldsymbol{G} \cdot \boldsymbol{V} d\Gamma + \int_{\Gamma_1} \boldsymbol{G}_1 \cdot \boldsymbol{V} d\Gamma + \int_{\Gamma_2} \boldsymbol{G}_2 \cdot \boldsymbol{V} d\Gamma \ , \tag{23}$$

$$\boldsymbol{G} = \{f_i(v_i + w_i) - e_{ijkl} v_{k.l} w_{i,j} + \Lambda\} \boldsymbol{n} \ , \tag{24}$$

$$\boldsymbol{G}_1 = \{P_{i,j} n_j (v_i + w_i) + P_i (v_{i,j} + w_{i,j}) n_j + P_i (v_i + w_i) \kappa\} \boldsymbol{n} , \tag{25}$$

$$\boldsymbol{G}_2 = \{p'(v_i + w_i) n_i + \mathrm{div}(p v_i + p w_i)\} \boldsymbol{n} \ . \tag{26}$$

Since the shape gradient function has been derived, the traction method can be applied.

4 Traction method and shape optimization system

The traction method [1] is a gradient method in a Hilbert space. In the traction method, the negative shape gradient function $-\boldsymbol{G}$ is applied in the normal direction to the design boundary as an external traction force, i.e., as a Neumann condition to vary the shape. We call this process the velocity analysis. The resultant displacement field (i.e., design velocity field) $\Delta s \boldsymbol{V}$ represents the amount of domain variation added to the original shape to update it. Using this method, the smooth domain variation that minimizes the objective functional can be obtained. By repeating the stress analysis and the adjoint analysis that yield the shape gradient function, the velocity analysis and the updating of the shape by $\Delta s\boldsymbol{V}$, the optimum shape can be obtained. The process of the optimization system based on this method is schematized in Fig. 3. Other advantages of this method are summarized as follows: (1) it is not necessary to parameterize the shape unlike the basis vector method, because all nodes on the design domain can be moved as the design variable, (2) it is not necessary to refine the mesh, because the entire domain can be mapped by the traction force, (3) it assures smooth boundary shapes without any zigzagging, because the elastic tensor serves as a smoother, (4) it can be easily implemented in combination with a commercial FEM code, which means it has generality and practical utility for actual design work. More details of the traction method involving the verification of smoothness are given in reference [6].

The governing equation of the velocity analysis with the Neumann condition is given as

$$a(\boldsymbol{V},\boldsymbol{w}) = -l_G(\boldsymbol{w}), \quad \forall \boldsymbol{w} \in C_\Theta \ . \tag{27}$$

Equation (27) can be solved by a standard finite element analysis.

The mean curvature κ in eqn. (25) for the C_0-continuity surface on the linear solid elements of a FE model was approximated by differentiating the Bezier surface obtained by the method of least squares. For a quadratic solid element, it can be calculated by using its shape function.

It can be confirmed that the domain variation $\boldsymbol{V}$ determined by the velocity analysis reduces the Lagrangian functional L. When the state equation, the adjoint equation and the constraints are satisfied, the perturbation expansion of L can be written as

$$\Delta L = l_G(\Delta s\boldsymbol{V}) + O(|\Delta s|) . \tag{28}$$

Substituting eqn. (27) into eqn. (28) and taking into account the positive definitiveness of $a(\boldsymbol{v},\boldsymbol{w})$, based on the positive definitiveness of the elastic tensor e_{ijkl}

$$\exists \alpha > 0 : a(\xi,\xi) \geq \alpha \|\xi\|^2 , \forall \xi \in U , \tag{29}$$

the following relationship is obtained when Δs is sufficiently small:

$$\Delta L = -a(\Delta s\boldsymbol{V}, \Delta s\boldsymbol{V}) < 0 \ . \tag{30}$$

This relationship definitely reduces the Lagrangian functional in the process of changing the domain using the velocity field $\boldsymbol{V}$ determined by eqn. (27). By repeating the stress analysis for evaluating the shape gradient function, the velocity analysis and the updating of the shape by $\Delta s\boldsymbol{V}$, the objective functional is minimized, resulting in the smooth optimum shape.

5 Results of shape optimization

To confirm the validity of the proposed solution, it was applied to four design problems. In all four examples, it was assumed that the body forces, the surface

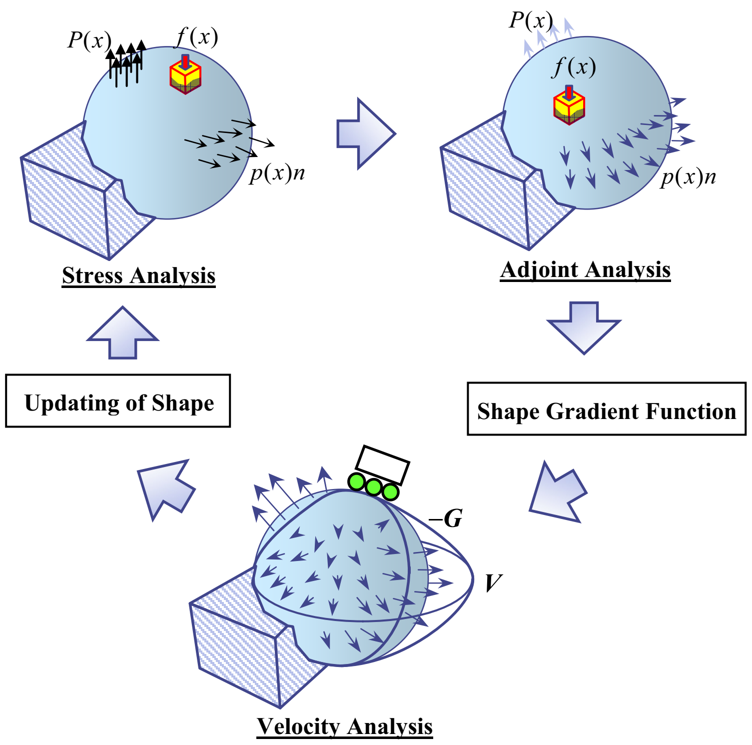

Figure 3: Schematic diagram of traction method.

forces and the pressure were constant with respect to s within the space ($\boldsymbol{f}' = \boldsymbol{P}' = p'(\boldsymbol{x})\boldsymbol{n} = 0$).

5.1 Short span beam problem

A short span beam fixed at both ends was optimized. This short span beam is subjected to both shearing stress and bending stress. The boundary conditions of the stress analysis and of the velocity analysis are shown in Fig. 4(a) and (b), respectively. In the stress analysis, downward uniformly distributed loads P ($P_{i,j} = 0$, or $\dot{P} = 0$) were applied on the upper and lower variable Neumann boundaries, where the design boundaries to be optimized were located. In the velocity analysis, the length and width were kept constant. A constant volume constraint was applied. The initial shape and the optimal shape that was calculated by using eqn. (24) (except the term for body force $f_i(v_i + w_i)$) and eqn. (25) as the shape gradient function, are shown respectively in Fig. 5(a) and (c). For comparison, the final shape calculated by only using the strain energy density (SED) and Λ in eqn. (24) as the shape gradient function is shown in Fig. 5(b), since SED is often used in place of the shape gradient function as a convenient index for the rigidity design. It is seen that both shapes (b) and (c) obtained have smooth boundaries. Figure 6 shows iteration histories of the volume and compliance in the optimization process. The values are normalized to the values of the initial shape. Both compliances are minimized while satisfying the volume constraint, but the rate of reduction is different; the rate for (b) is 17% while that for (c) is 19%. It is also seen that the optimal shape (c) is clearly different from the shape (b) at the beam center. These results confirm the effectiveness of the derived shape gradient function and our solution.

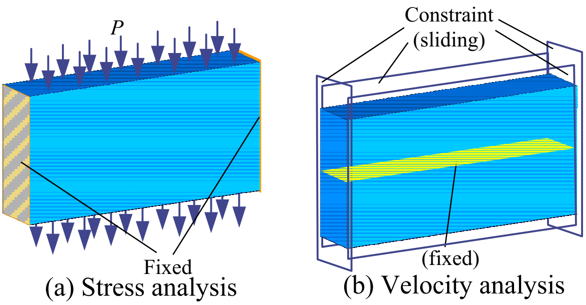

Figure 4: Boundary conditions for short span beam problem.

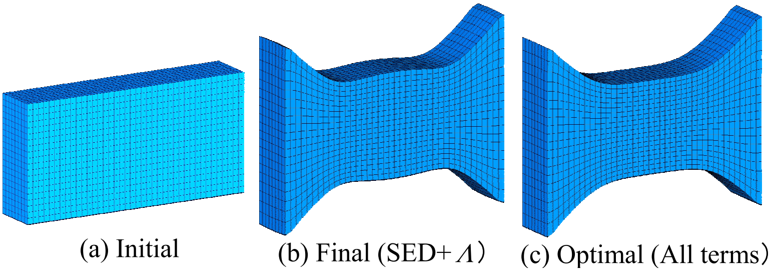

Figure 5: Calculated results of short span beam problem.

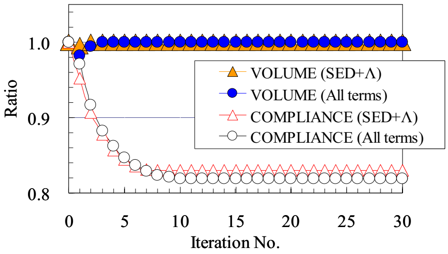

Figure 6: Iteration histories of short span beam problem.

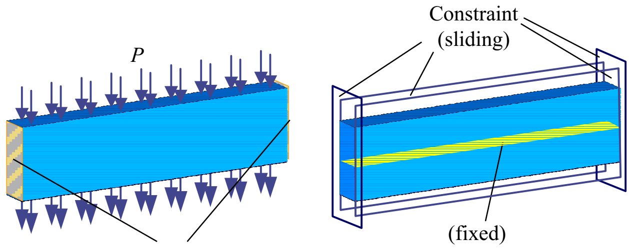

(a) Stress analysis (b) Velocity analysis

Figure 7: Boundary conditions for long span beam problem.

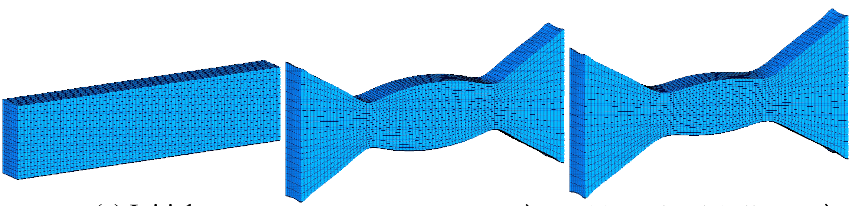

(a) Initial (b) Final (SED+Λ) (c) Optimal (All terms)

Figure 8: Calculated results of long span beam problem.

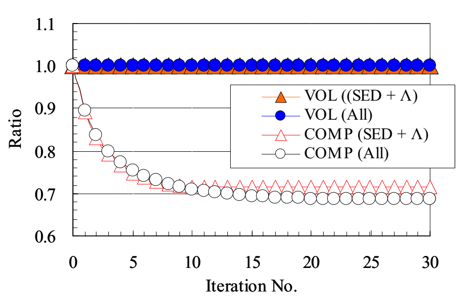

Figure 9: Iteration histories of long span beam problem.

5.2 Long span beam problem

A long span beam fixed at both ends was optimized. This long span beam is mainly subjected to bending stress. The boundary conditions and optimization conditions were the same as the short span beam problem as shown in Fig. 7(a) and (b). The initial shape and the optimal shape that was calculated by using eqn. (24) (except the term for body force $f_i(v_i + w_i)$) and eqn. (25) as the shape gradient function, are shown respectively in Fig. 8(a) and (c). For comparison, the final shape calculated by only using the strain energy density (SED) and Λ in eqn. (24) as the shape gradient function is shown in Fig. 8(b). It is seen that both shapes (b) and (c) obtained have smooth boundaries. It is also seen that the optimal shape (c) is clearly different from the shape (b). Figure 9 shows iteration histories of the volume and compliance in the optimization process. Both compliances are minimized while satisfying the volume constraint, but the rate of reduction is different; the rate for (b) is 28% while that for (c) is 32%. These results also confirm the effectiveness of the derived shape gradient function.

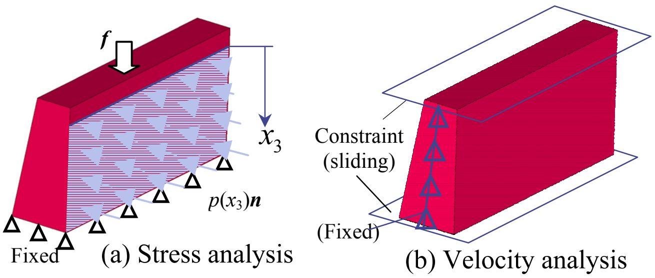

Figure 10: Boundary conditions of dam problem.

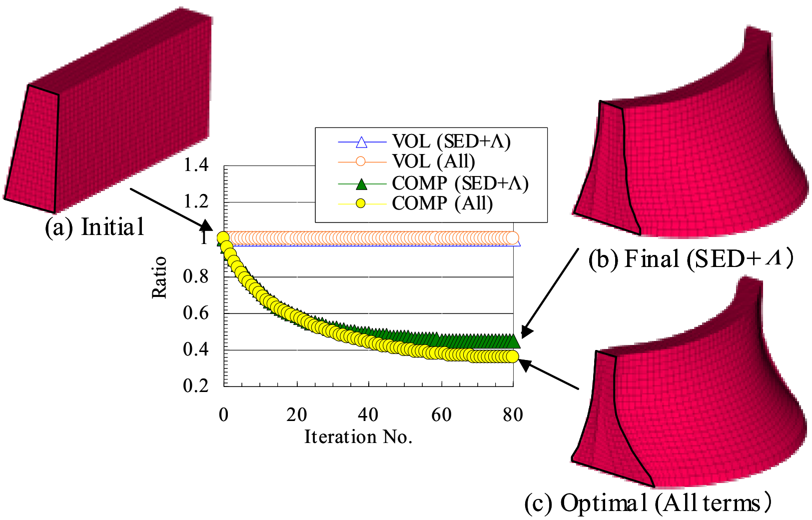

Figure 11: Iteration histories and obtained shapes of dam problem.

5.3 Dam problem

Boundary conditions for the shape optimization of a dam model are shown in Fig. 10. In the stress analysis, the bottom of the dam was fixed, and a hydro-pressure $p(x_3)\boldsymbol{n} = \rho g x_3 \boldsymbol{n}$ (ρ: density, g: gravity acceleration) and the gravity force $\boldsymbol{f}$ were applied (assuming $p'(x_3) = 0, \boldsymbol{f}' = 0$) as shown in Fig. 10(a). In the velocity analysis, the height and width were kept constant and the center lines of both side boundaries were fixed. The boundary with the hydro-pressure and the opposite boundary were set as the design boundaries to be optimised as shown in (b). A constant volume was set as the constraint. The iteration histories and obtained shapes are shown in Fig. 11, where (a) is the initial shape and (c) is the optimal shape obtained with eqns. (24) and (26) as the shape gradient function. To make the same comparison as in the beam problem, the final shape calculated by only using SED and Λ in eqn. (24) is shown in Fig. 11(b). It is seen that a smooth converged shape was obtained in each case and that the cross-section shapes are different. In both shapes, the objective functional decreased monotonically while satisfying the volume constraint. The compliance was reduced by 55% in (b) and by 64% in (c). These results also confirm the effectiveness our solution.

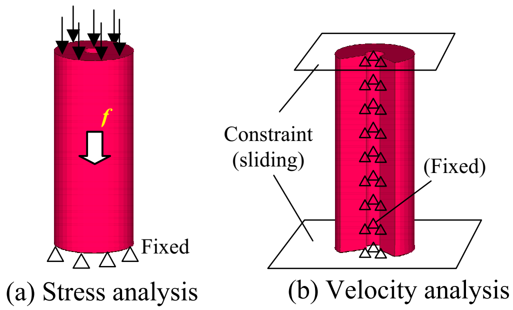

Figure 12: Boundary conditions of tower problem.

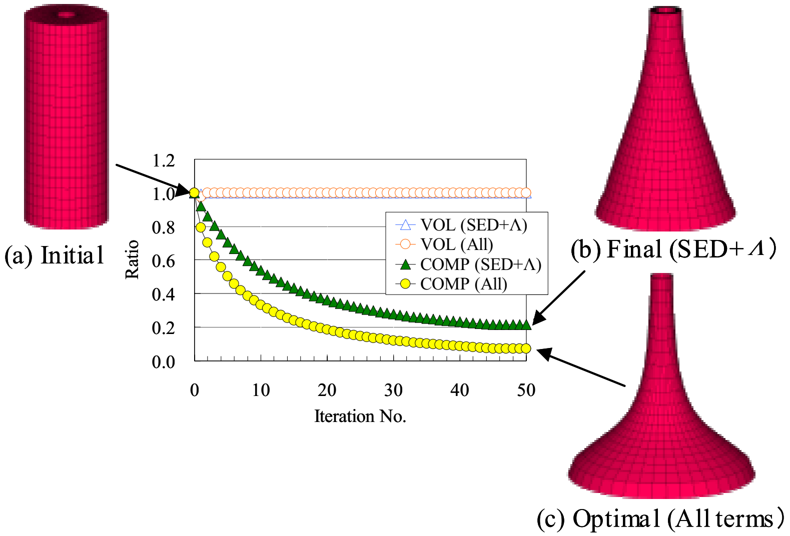

Figure 13: Iteration histories and obtained shapes of tower problem.

5.4 Tower problem

A cylindrical tower under the gravity force **f** and downward nodal forces at the top surface as shown in Fig. 12(a) was optimized. In the velocity analysis, the height was kept constant, and the inside hole was fixed as shown in Fig. 12(b). The volume remained constant as the constraint. The iteration histories and obtained shapes are shown in Fig. 13, where (c) is the optimal shape obtained by using all the terms in eqn. (24) as the shape gradient function. Depending on the magnitude of the shape gradient function, the upper portion contracted, and the lower portion was expanded. (b) is the final shape calculated by only using SED and Λ in eqn. (24) for comparison. The compliance was reduced by 80% in (b) and by 95% in (c) as expected, while satisfying the volume constraint.

6 Conclusion

In this paper we have proposed a practical solution to the shape optimization problem of solid structures. With this solution, the optimum free-form and smooth shape can be determined without any parameterization of the shape for optimization. For the rigidity design of a solid structure, a compliance minimization problem subject to a volume constraint is formulated as a non-parametric shape optimization problem. In order to reduce the total amount of applied loads, it is considered that the Neumann boundary is allowed to vary. The shape gradient function for this problem is derived, and is applied to the traction method. The validity and practical utility of this solution were verified based on the results obtained for four design examples.

References

[1] Azegami H. and Wu Z. C., Domain Optimization Analysis in Linear Elastic Problems (Approach Using Traction Method), *JSME Int. J.*, Series A, 39(2), pp. 272-278, 1996.

[2] Shimoda M., Azegami H. and Sakurai T., Traction Method Approach to Optimal Shape Design Problems, SAE Transactions, Journal of Passenger Cars, 106 (6), pp. 2355-2365, 1998.

[3] Shimoda M. and Tsuji J., Non-parametric Shape Optimization Method for Rigidity Design of Automotive Sheet Metal Structures, SAE Transactions, Journal of Passenger Cars, SAE Paper 200601-0584, 2006.

[4] Sokolowski J. and Zolesio J. P., *Introduction to Shape Optimization -Shape Sensitivity Analysis*, Springer-Verlag: New York, 1991.

[5] Haug E. J., Choi K. K. and Komkov V., *Design Sensitivity Analysis of Structural Systems*, Academic Press, Orlando, 1986.

[6] Azegami H., Kaizu S., Shimoda M. and Katamine E., Irregularity of Shape Optimization Problems and an Improvement Technique, in *Computer Aided Optimum Design of Structures V*, Hernandez V. S. and Brebbia C. A. (eds), Computational Mechanics Publications, Southampton, pp. 309-326, 1997.